IJMMM International Journal of Minerals, Metallurgy and Materials 矿物冶金与材料学报（英文版）

Growth kinetics of titanium carbide coating by molten salt synthesis process on graphite sheet surface

Xiaoyu Shi, Chongxiao Guo, Jiamiao Ni, Songsong Yao, Liqiang Wang, Yue Liu, and Tongxiang Fan

Cite this article as:
Xiaoyu Shi, Chongxiao Guo, Jiamiao Ni, Songsong Yao, Liqiang Wang, Yue Liu, and Tongxiang Fan, Growth kinetics of titanium carbide coating by molten salt synthesis process on graphite sheet surface, *Int. J. Miner. Metall. Mater.*, 31(2024), No. 8, pp. 1858-1864. https://doi.org/10.1007/s12613-023-2749-8

INTERNATIONAL JOURNAL OF
Minerals, Metallurgy and Materials

Volume 31, Number 8, August 2024
Page 1858

Research Article https://doi.org/10.1007/s12613-023-2749-8

Growth kinetics of titanium carbide coating by molten salt synthesis process on graphite sheet surface

Xiaoyu Shi, *Chongxiao Guo*, *Jiamiao Ni*, *Songsong Yao*, *Liqiang Wang*, *Yue Liu*✉, *and Tongxiang Fan*✉

State Key Lab of Metal Matrix Composites, School of Materials Science and Engineering, Shanghai Jiao Tong University, Shanghai 200240, China
(Received: 19 July 2023; revised: 13 September 2023; accepted: 15 September 2023)

Abstract: The synthesis of carbide coatings on graphite substrates using molten salt synthesis (MSS), has garnered significant interest due to its cost-effective nature. This study investigates the reaction process and growth kinetics involved in MSS, shedding light on key aspects of the process. The involvement of Ti powder through liquid-phase mass transfer is revealed, where the diffusion distance and quantity of Ti powder play a crucial role in determining the reaction rate by influencing the C content gradient on both sides of the carbide. Furthermore, the growth kinetics of the carbide coating are predominantly governed by the diffusion behavior of C within the carbide layer, rather than the chemical reaction rate. To analyze the kinetics, the thickness of the carbide layer is measured with respect to heat treatment time and temperature, unveiling a parabolic relationship within the temperature range of 700–1300°C. The estimated activation energy for the reaction is determined to be 179283 $J \cdot mol^{-1}$. These findings offer valuable insights into the synthesis of carbide coatings via MSS, facilitating their optimization and enhancing our understanding of their growth mechanisms and properties for various applications.

Keywords: titanium carbide; graphite; molten salt; kinetic analysis

1. Introduction

Carbon-based materials, such as carbon fiber (C_f), diamond, and graphite, are renowned for their low density and high mechanical strength at elevated temperatures, rendering them suitable for the applications in extreme environments and ultra-high-temperature [1–8]. However, their susceptibility to oxidation poses a challenge, necessitating protective measures in harsh conditions is thus required [9–12]. To mitigate this concern, surface modification coatings based on refractory carbides have been extensively employed for carbon-based materials. These carbides exhibit exceptional chemical compatibility with carbon and possess remarkably high melting points, thereby effectively enhancing the oxidation resistance of carbon-based materials [13–16].

Traditional coating preparation techniques, such as chemical vapor deposition (CVD) and physical vapor deposition (PVD), require high vacuum levels, controlled reaction gases, and complex, expensive equipment [17–25]. Consequently, the cost of producing carbide coatings using these methods is substantial. An alternative approach is molten salt synthesis (MSS). The MSS process involves the diffusion of refractory metal atoms within a liquid phase and chemical reaction between these atoms and the surface of carbon materials. As a result, it may offer a faster, simpler, and more cost-effective method for synthesizing refractory carbides. MSS has been successfully utilized to coat various refractory carbides, including TiC, ZrC, SiC, and TaC, onto carbon materials [26–32]. Extensive researches have demonstrated that carbides synthesized via MSS exhibit favorable mechanical properties and enhance the oxidation resistance of carbon-based materials. For instance, Constantin *et al.* [33] reported the spontaneous formation of multi-layered carbide coatings on carbon fiber surfaces using MSS, which displayed exceptional resistance to harsh environments. Behboudi *et al.* [34] reported the *in-situ* synthesis of TiC coatings on graphite surfaces via MSS, leading to improved oxidation resistance of graphite flakes. These studies emphasize the potential of MSS as a straightforward and cost-effective method for synthesizing refractory carbide coatings [35–36].

The quantitative analysis of factors influencing the growth kinetics of carbide coatings in the MSS reaction remains largely unexplored. Specifically, in the case of widely studied TiC coatings, the growth kinetics of carbide layers are commonly attributed to the rate of carbon (C) diffusion, as C exhibits a significantly higher diffusion coefficient in titanium carbide (TiC) than in titanium. However, other researches have reported large discrepancies regarding the effective diffusion growth coefficients of TiC. Constantin *et al.* [33] and Behboudi *et al.* [34] found that the effective diffusion growth coefficients of TiC is smaller than the diffusion coefficient of C in TiC. These results suggested that other factors may be involved in the growth kinetics of carbide coatings. Given that growth kinetics dictate the synthesis of

✉ Corresponding authors: Yue Liu E-mail: yliu23@sjtu.edu.cn; Tongxiang Fan E-mail: txfan@sjtu.edu.cn

carbide coatings, a comprehensive study on the reaction kinetics of MSS synthesized carbides is essential to facilitate the rational design of carbide coatings with desirable properties.

This study aims to investigate the MSS of TiC as a representative case for carbide synthesis. Initially, a well-defined and uniform TiC coating was synthesized on the surface of a graphite block using the MSS process. The specific role and impact of titanium particles presented in the molten salt medium on the growth of the carbide coating were thoroughly examined. Subsequently, a diffusion theory model was developed to comprehensively elucidate the growth kinetics of TiC layers during the MSS process. These investigations are conducted to achieve a deeper understanding of the underlying mechanisms governing MSS carbide synthesis. This, in turn, enables improved control and optimization of carbide coating properties.

2. Methodology

Isostatic graphite sheets, with a thickness of 2 mm and a purity exceeding 99%, were chosen as the substrate material for synthesizing TiC coatings. The molten salt medium used in the process consisted of high-purity chloride salts, namely KCl (>99.5% purity) and NaCl (>99.5% purity). The mass ratio of Ti to NaCl to KCl was adjusted within the range of Ti : NaCl : KCl = (0.25–4):20:25. To initiate the synthesis, the fine titanium powder and the chloride salts were thoroughly mixed to achieve a homogeneous distribution. The mixture was then placed in an alumina crucible. Careful embedding of the graphite sheet into the mixture was performed to ensure proper contact between the graphite sheet and the mixture components. The entire assembly was subjected to heat treatment in a tube furnace at a temperature range of 700–1000°C under an argon atmosphere. The heating and cooling rates were maintained at approximately 5°C/min to ensure controlled thermal conditions. After the completion of the heat treatment, the assembly was allowed to cool naturally to room temperature. To remove the molten salt, the graphite sheet was extracted from the assembly and treated with water to dissolve the salt. The extracted graphite sheet was labeled to distinguish between the top and bottom sides and then thoroughly rinsed with distilled water to eliminate any remaining salt residues.

X-ray diffraction (XRD) analysis was conducted on a Rigaku Mini Flex 600 instrument to determine the phase composition of both the graphite sheet and the synthesized coating. XRD measurements were carried out in the 2θ range of 20°–80° using monochromatic Cu K_α radiation at 40 kV and 15 mA. The obtained XRD data provided valuable insights into the crystalline structure of the samples. To analyze the microstructure and composition, samples were examined using a RISE-MAGNA scanning electron microscope (SEM) equipped with an energy-dispersive X-ray spectrometer (EDS). This combination allowed for the characterization of the sample's surface morphology, as well as the elemental composition analysis. Cross-sectional views of the coated graphite were obtained by longitudinally fracturing the graphite sheets under compressive forces, providing a detailed view of the coating structure. These characterization techniques provided a comprehensive understanding of the microstructure, phase composition, and elemental distribution of the synthesized TiC coatings on isostatic graphite sheets. This facilitated further analysis and evaluation of the coating's properties.

3. Results and discussion

3.1. Growth of TiC coating

The growth of TiC coatings on graphite surfaces was investigated by heat treatment at 700, 750, 850, and 950°C for 30 min. XRD analysis of the graphite sample after molten salt treatment revealed only the presence of the graphite matrix phase and the TiC coating, with no detection of other phases such as Ti or TiO_2 (Fig. 1(a)). The relative peak intensity of the TiC phase increased with increasing temperature, indicating that temperature is a significant factor affecting the synthesis rate of TiC. A higher peak intensity also suggested that the generated TiC was thicker. Fig. 1(b) shows a cross-sectional view of the fracture surface of graphite after molten salt treatment at 850°C. EDS analysis confirmed the distribution of Ti and C in these regions. Plan-view observations (Fig. 1(c)–(f)) revealed a uniform distribution of Ti and C elements with no aggregation or exposed areas. Statistical analysis of the atomic ratio of Ti to C indicated an average phase composition of approximately $TiC_{0.76}$. These results suggest that the generated TiC phase exhibits a certain degree of content variation, consistent with previous experimental findings reported by Constantin *et al.* [33] and Behboudi *et al.* [34]. Overall, these results demonstrate that the TiC coating grown on graphite surfaces via molten salt treatment is uniform and free of voids and cracks.

To further elucidate the reaction process underlying the synthesis of TiC in molten salt, residual Ti powder was obtained by cleaning the original and post-treatment mixtures. Fig. 2(a) shows the morphology of Ti powder before and after heat treatment at temperature ranging from 700 to 950°C. The original Ti powder exhibited sharp edges and corners and a dense polyhedral morphology. In contrast, heat treatment in molten salt resulted in the gradual disappearance of these features and the emergence of dissolution holes in the previously dense block body. The obtained results support the conclusion that titanium powder exhibits a reaction and dissolution behavior in molten salt. Through the diffusion of titanium in the liquid phase, the growth of TiC coatings is facilitated. Straumanis *et al.* [37] found that titanium will react with chloride salts to form low-valent chlorides of titanium at high temperatures. These low-valent chlorides can dissolve in chloride salts, enabling the diffusion of titanium in the liquid phase. Experimental observations revealed that the color of the mixed chloride salts changed from white to green after treatment with titanium powder. Additionally, gas generation and the production of a strongly reductive sub-

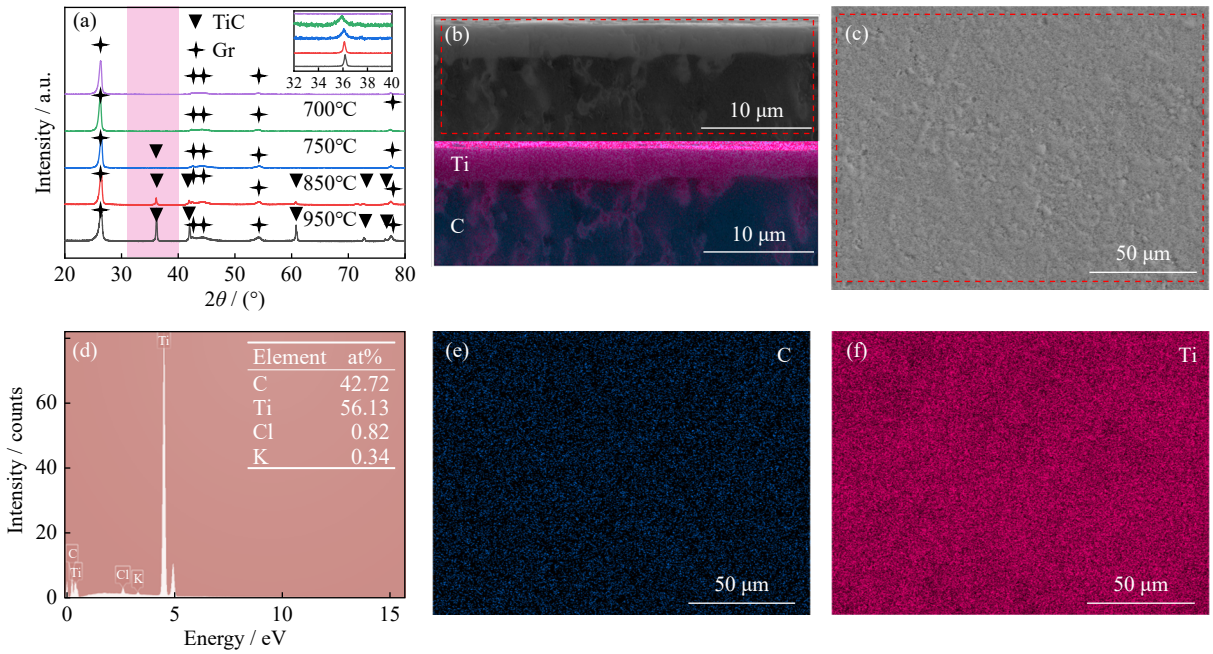

Fig. 1. Phase and microstructure of TiC coating: (a) effect of temperature on TiC synthesis; (b–f) representative microstructures and EDS surface scan images.

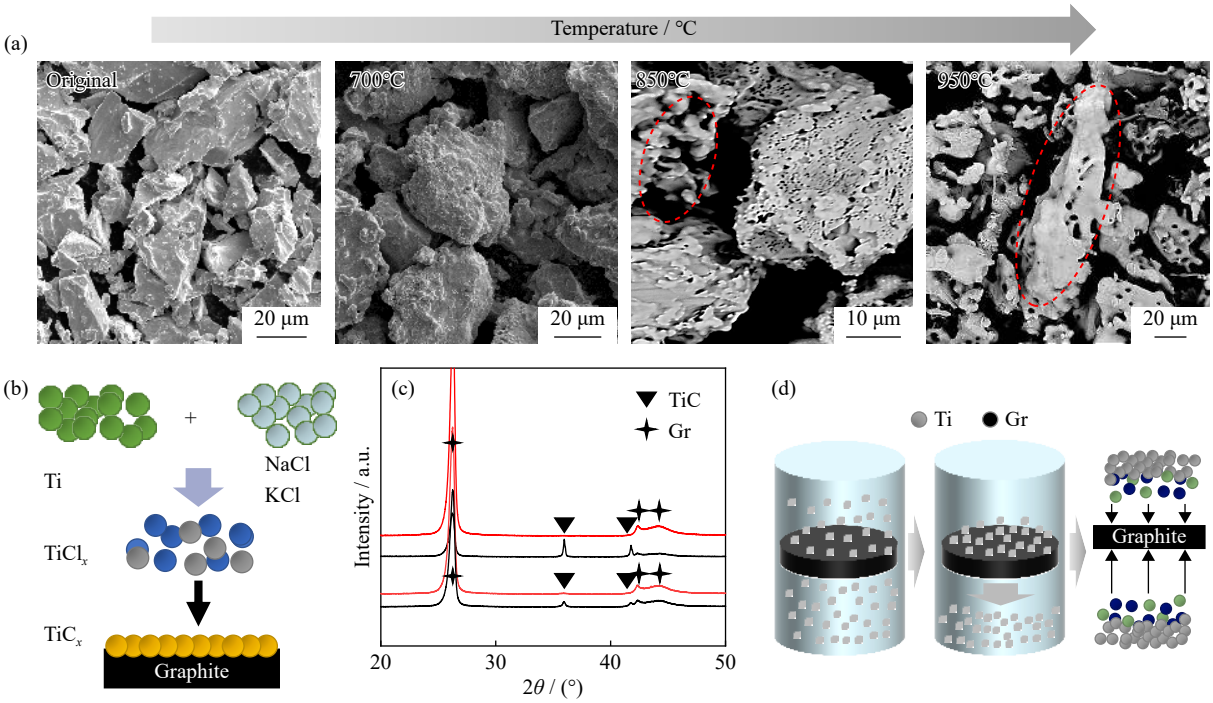

Fig. 2. Influence of temperature and diffusion distance on the reaction process: (a) partial solubility of Ti powder in molten salt; (b) schematic representation of titanium powder reaction; (c) inhibition of TiC growth with increasing diffusion distance; (d) impact of Ti powder distance on mass transfer.

stance were observed when the green salt came into contact with water. These experimental phenomena indicate the presence of a green titanium compound in the treated chloride salt, which acts as a highly reducing agent.

The overall reaction process is depicted in Fig. 2(b): Ti powder reacts with the mixed chloride salts, resulting in the formation of low-valent titanium compounds. These compounds then diffuse to the graphite surface within the liquid molten salt and react with C, ultimately leading to the formation of TiC coatings. To investigate the potential influence of the reaction distance between graphite and titanium powder on the rate of TiC formation, a comparison was made between the two sides of graphite sheets under the effects of gravity segregation. The XRD results of the treated graphite sheets, following heat treatment at 750 and 850°C for 30 min, are depicted in Fig. 2(c). The XRD results for the bottom side of the graphite sheet are labeled as 750°C-B and 850°C-B, represented by red lines, while the top side results are represented by black lines. Notably, distinct TiC diffraction peaks are observed on the top side of the graphite, while no such

peaks are observed on the bottom side. During the experimental process, gravity segregation led to an increase in the distance between the titanium powder and the bottom side of the graphite (less than 3 mm), as illustrated in Fig. 2(d). These findings suggest that even a slight increase in distance between Ti and graphite can significantly impact the reaction rate of TiC formation.

3.2. Growth kinetics of titanium carbide

A schematic diagram illustrating the diffusion analysis in the reaction system containing TiC is presented in Fig. 3(a) and (b). In this molten salt system, C does not exhibit dissolution or diffusion behavior and TiC grows on the surface of graphite. Therefore, the main research object of the diffusion model is the carbide layer. The reaction between molten salt and TiC occurs on the Ti-rich side, where Ti atoms diffuse through the existing TiC layer towards the graphite substrate. On the carbon-rich side, C atoms diffuse through TiC towards its surface. Generally, C atoms have a significantly higher diffusion coefficient (D) in TiC than Ti atoms due to their interstitial diffusion mechanism. Therefore, the growth rate of the carbide layer is primarily determined by the speed of C diffusion through TiC towards the graphite surface, and the contribution from Ti atoms diffusion can be neglected [38].

The diffusion process of C through the carbide layer towards its surface can be described using solid-state diffusion theory. Assuming a constant C content in TiC on the molten salt side, the growth of TiC on the graphite surface can be considered as a diffusion process in a semi-infinite model. The C content curve for the system is depicted in Fig. 3(b). At the interfaces on both sides of TiC, the C content refers to the C solubility in the binary phase diagram for Ti–C. The TiC in contact with graphite has the highest C content (ρ_0), which is close to that of pure TiC. On the molten salt contact side, the C content (ρ_s) in TiC may remain constant within the range of TiC to $TiC_{0.5}$. For a typical semi-infinite diffusion couple, the solution of the diffusion equation for C content and diffusion time can be obtained:

$$\frac{\rho_0-\rho(x,\,t)}{\rho_0-\rho_s}=\mathrm{erf}\left(\frac{x}{2\sqrt{Dt}}\right)=A \tag{1}$$

where D is the diffusion coefficient ($cm^2 \cdot s^{-1}$), t is the diffusion time (s), and x is the diffusion distance (cm). By taking the approximation of Eq. (1), we obtain a simplified equation:

$$A\approx\left(\frac{x}{2\sqrt{Dt}}\right) \tag{2}$$

Combining Eqs. (1) and (2), we obtain expression for thickness of carbide coating as Eq. (3),

$$x=2A(\rho_s)\sqrt{Dt},\quad 0.5\gg A(\rho_s)>0 \tag{3}$$

Assuming that C content ρ_s on molten salt contact side for carbides is a function of proportion of titanium powder in salt:

$$\rho_s=f(C_{Ti})\quad(\rho_0>\rho_s\geq\rho_{TiC_{0.5}}) \tag{4}$$

where C_{Ti} represents the content of titanium in the molten salt. Thus, we obtain expression relating proportion variable for titanium to thickness of carbides:

$$x=2A\,(C_{Ti})\sqrt{Dt} \tag{5}$$

where $A\,(C_{Ti})$ is a function related to C_{Ti}.

In the experimental verification of the $A\,(C_{Ti})$ section, we utilized molten salts with varying proportions of titanium powder (mass ratio of Ti : NaCl : KCl = (0.25–4):20:25) for the heat treatment of graphite at 850°C. In order to exclude the influence of the distance between the reactants, we carried out a kinetic analysis of the TiC thickness on the top side of the graphite sheet. As depicted in Fig. 4(a)–(e), the data suggests a significant correlation between the proportion of Ti and the thickness of the carbide layer. To ensure sufficient consumption of titanium powder and avoid significant differences in coating thickness, we observed the remaining amount of titanium powder in the molten salt after growth. The results revealed the presence of residual titanium powder in all proportions of the molten salt, indicating an adequate quantity of titanium powder. The titanium powder influences the carbide thickness by affecting the C content on the carbide surface. Fig. 4(f) clearly illustrates the dependence of carbide thickness on the proportion of titanium powder in the molten salt. It is evident that when the titanium proportion is low, an increase in the proportion of titanium leads to a rapid increase in carbide thickness. This can be attributed to the consumption of C atoms on the carbide surface as the titanium proportion increases, resulting in a higher C content gradient on both sides and facilitating carbide growth. However, when the C content on the carbide surface ap-

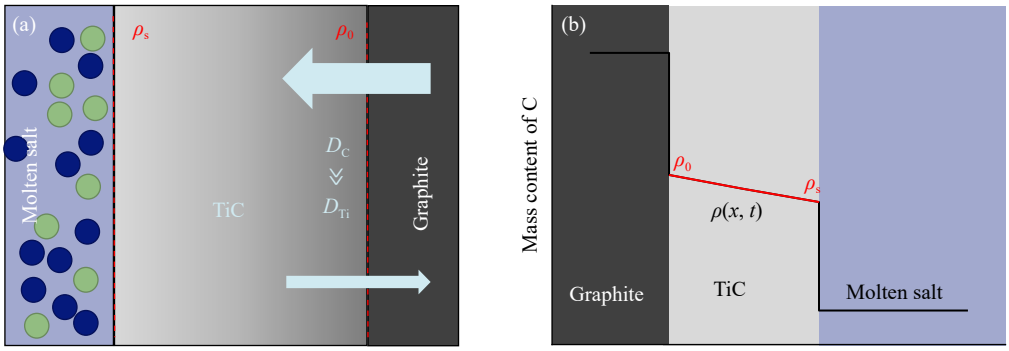

Fig. 3. Diffusion reaction kinetics model of coating: (a) schematic diagram of coating diffusion model; (b) C content distribution in reaction diffusion model.

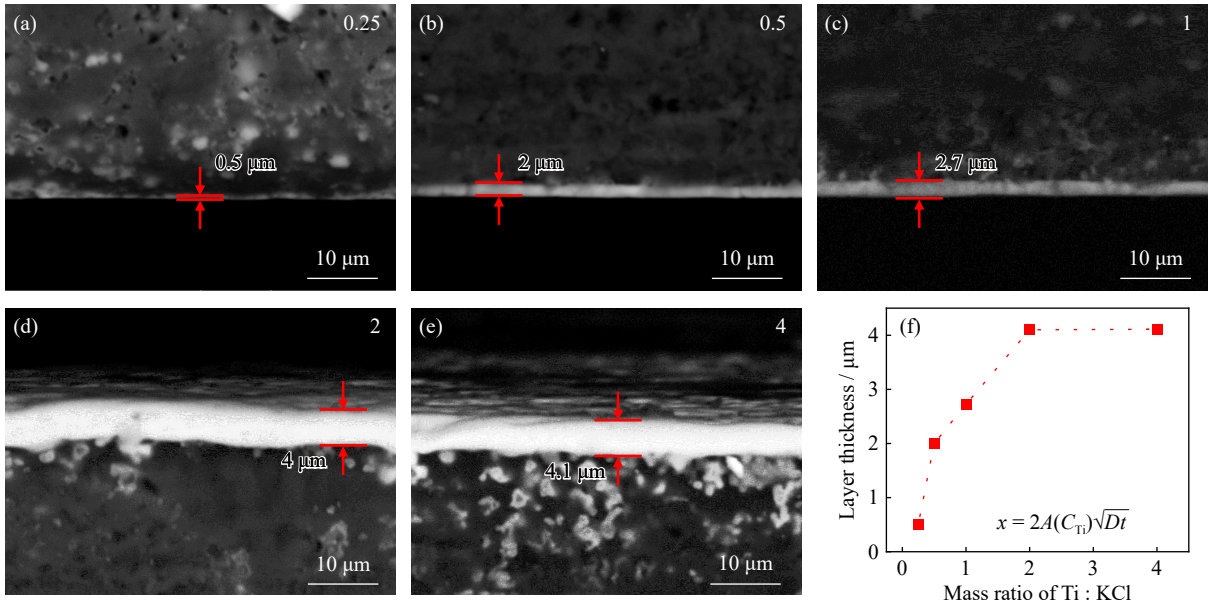

Fig. 4. Influence of titanium solubility in molten salt on coating growth: comparison of coating growth thickness with Ti : C mass ratios of (a) 0.25, (b) 0.5, (c) 1, (d) 2, and (e) 4; (f) TiC thickness growth and stabilization with increasing Ti content ratio.

proaches its limit value (close to $TiC_{0.5}$), further increases in the titanium proportion do not alter the C content gradient on both sides and therefore cannot affect the carbide thickness.

For the growth of carbide coatings, it is important to ensure a sufficient proportion of Ti to achieve the maximum difference in C content gradient on both sides of the carbide coating. Under this circumstance, $A(C_{Ti}) = 0.5$. We can obtain the relationship between coating thickness and diffusion coefficient and time:

$$x = \sqrt{Dt} \tag{6}$$

where x represents the coating thickness (cm), D represents the diffusion coefficient and/or growth rate constant ($cm^2 \cdot s^{-1}$), and t represents the heat treatment time (s). Fig. 5(a) and (b) shows the fitting results of layer thickness versus treatment time at different temperatures using linear and parabolic equations, respectively. The correlation coefficient (R^2) for parabolic fitting is 0.99, which is significantly higher than that for linear fitting at 0.89. This result indicates that there is a parabolic relationship between layer thickness and heat treatment time, which is in good agreement with the relationship shown by the equation. This further confirms that carbide growth is controlled by C diffusion.

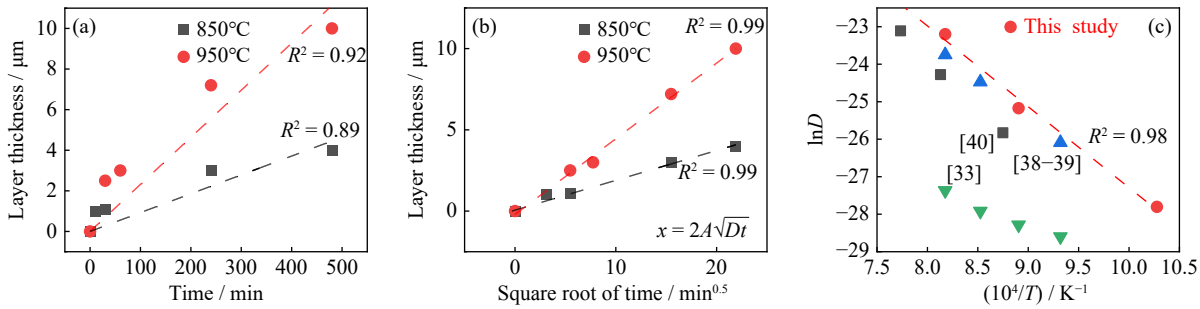

Fig. 5. Diffusion kinetics of C atoms in coatings: (a) linear fitting and (b) parabolic fitting equations for the relationship between TiC coating thickness and time; (c) comparison of diffusion coefficients of C in different studies.

According to the Eq. (6), the diffusion coefficient of C is calculated. At 700, 900, and 950°C, the diffusion coefficient of C (D_C) in TiC was found to be 8.40×10^{-13}, 1.16×10^{-11}, and 8.56×10^{-11} $cm^2 \cdot s^{-1}$, respectively. In addition, the correlation between diffusion coefficient (D) and process temperature (T) is shown in Fig. 5(c). Studies have been conducted on the diffusion growth kinetics of carbon during the diffusion bonding of titanium alloy with steel [38–39] and carbon graphite [40]. Our findings are consistent with the reported data on the diffusion coefficient of carbon, which is significantly larger than the growth coefficient of TiC obtained through Constantin's molten salt method [33]. This may be due to the fact that in Constantin's MSS research [33], the reaction ratio of Ti to C_f was relatively small, resulting in an insufficient C content gradient on both sides of the carbide ($A(C_{Ti}) < 0.5$), thus exhibiting a parabolic growth relationship but with a smaller apparent diffusion coefficient. The relationships among D, activation energy (Q), and the process temperature (T) could be expressed as an Arrhenius equation [40],

$$D = D_0 \exp\left(-\frac{Q}{RT}\right) \tag{7}$$

where D_0 is the pre-exponential constant and R is the gas constant equal to 8.314 J·mol^{-1}·K^{-1}. Eq. (8) could be expressed in the form of a natural logarithm as follows,

$$\ln D = \ln D_0 - \frac{Q}{RT} \tag{8}$$

By fitting the experimental results using the Eq. (8), we obtained a diffusion activation energy of 179.283 kJ/mol and D_0 = 0.003254 m^2·s^{-1}. The relationship between carbide layer thickness and processing temperature and time can then be expressed as follows:

$$x = \sqrt{D_0 \exp\left(-\frac{Q}{RT}\right) t} \tag{9}$$

Eq. (9) can be used to predict the carbide thickness at different processing temperatures and times (when Ti is sufficient). To further verify its accuracy and applicability at other temperatures, heat treatment was performed at 1100 and 1300°C for 240 min. The predicted thicknesses were 26.2 and 72.2 μm, respectively, while the corresponding experimental values were 28.6 and 63.4 μm. The deviations between predicted values and experimental values were 9.2% and 12.2%, indicating that thickness can be accurately predicted by temperature and time within the range of 700–1300°C. From these results, we can conclude that (1) the growth kinetics of carbides is controlled by C diffusion; (2) carbide thickness follows a typical parabolic relationship with time; (3) the diffusion coefficient also follows an Arrhenius equation with temperature.

4. Conclusion

In conclusion, a dense and uniform carbide coating was successfully grown on a graphite substrate using the MSS method. The presence of Ti powder played a crucial role in facilitating the liquid-phase mass transfer of Ti atoms, resulting in the formation of TiC. The growth rate of TiC was primarily controlled by the diffusion of C atoms driven by the difference in C content gradient on both sides of the carbide. The Ti content ratio influenced the carbide growth rate by affecting the C content on the carbide surface. The experimental results confirmed the diffusion parabolic kinetics of TiC growth, with diffusion coefficients and activation energies consistent with values reported in other systems. These findings provide valuable insights into the growth mechanisms of carbide coatings synthesized via the molten salt method.

Acknowledgements

This work was financially supported by the National Natural Science Foundation of China (No. 52171144) and the Fundamental Research Special Zone Program of Shanghai Jiao Tong University (No. 21TQ1400215).

Conflict of Interest

On behalf of all authors, the corresponding author states that there is no conflict of interest.

References

[1] P.P. Wang, G.Q. Chen, W.J. Li, *et al*., Microstructural evolution and thermal conductivity of diamond/Al composites during thermal cycling, *Int. J. Miner. Metall. Mater.*, 28(2021), No. 11, p. 1821.

[2] H.D. Zhang, J.J. Zhang, Y. Liu, F. Zhang, T.X. Fan, and D. Zhang, Unveiling the interfacial configuration in diamond/Cu composites by using statistical analysis of metallized diamond surface, *Scripta Mater.*, 152(2018), p. 84.

[3] Z.F. Hu, Y.C. Tong, M. Wang, J.B. Xu, and C. Yang, Rapid and low-cost carbon/carbon composites by using graphite slurry impregnated prepregs, *J. Eur. Ceram. Soc.*, 43(2023), No. 10, p. 4363.

[4] S. Chand, Review carbon fibers for composites, *J. Mater. Sci.*, 35(2000), No. 6, p. 1303.

[5] T.K. Das, P. Ghosh, and N.C. Das, Preparation, development, outcomes, and application versatility of carbon fiber-based polymer composites: A review, *Adv. Compos. Hybrid Mater.*, 2(2019), No. 2, p. 214.

[6] S. Zhang and W.E. Lee, Carbon containing castables: Current status and future prospects, *Br. Ceram. Trans.*, 101(2002), No. 1, p. 1.

[7] I.R. de Oliveira, A.R. Studart, V.C. Pandolfelli, and B.A. Menegazzo, Zero-cement refractory castables, *Am. Ceram. Soc. Bull.*, 81(2002), No. 12, p. 27.

[8] M.M. Harussani, S.M. Sapuan, G. Nadeem, T. Rafin, and W. Kirubaanand, Recent applications of carbon-based composites in defence industry: A review, *Def. Technol.*, 18(2022), No. 8, p. 1281.

[9] M. Yang, Y. Liu, T.X. Fan, and D. Zhang, Metal-graphene interfaces in epitaxial and bulk systems: A review, *Prog. Mater. Sci.*, 110(2020), art. No. 100652.

[10] T.X. Fan, Y. Liu, K.M. Yang, J. Song, and D. Zhang, Recent progress on interfacial structure optimization and their influencing mechanism of carbon reinforced metal matrix composites, *Acta Metall. Sin.*, 55(2019), No. 1, p. 16.

[11] J. Song, S.S. Yao, Q. Li, *et al*., Reorientation mechanisms of graphene coated copper{001} surfaces, *Metals*, 13(2023), No. 5, art. No. 910.

[12] C. Verdon, O. Szwedek, S. Jacques, A. Allemand, and Y. Le Petitcorps, Hafnium and silicon carbide multilayer coatings for the protection of carbon composites, *Surf. Coat. Technol.*, 230(2013), p. 124.

[13] M.P. Bacos, Carbon–carbon composites: Oxidation behavior and coatings protection, *J. Phys. IV*, 3(1993), No. C7, p. C7-1895.

[14] C. Friedrich, R. Gadow, and M. Speicher, Protective multilayer coatings for carbon–carbon composites, *Surf. Coat. Technol.*, 151-152(2002), p. 405.

[15] Z.L. Liu, C.J. Deng, C. Yu, J. Ding, and H.X. Zhu, Improving the anti-oxidation and water wettability of graphite through the design of coating structure for the preparation of Al_2O_3–SiC–C castables, *Ceram. Int.*, 49(2023), No. 17, p. 29104.

[16] C.L. Kuang, X. Wang, Z.L. Liu, *et al*., Nanocrystalline ZrC coated graphite and its effect on mechanical properties and thermal shock resistance of low-carbon Al_2O_3–C refractories, *Ceram. Int.*, 48(2022), No. 22, p. 33926.

[17] X. Yang, Q.Z. Huang, Z.A. Su, *et al*., Resistance to oxidation and ablation of SiC coating on graphite prepared by chemical vapor reaction, *Corros. Sci.*, 75(2013), p. 16.

[18] P. Zhu, P.P. Wang, P.Z. Shao, *et al*., Research progress in interface modification and thermal conduction behavior of diamond/metal composites, *Int. J. Miner. Metall. Mater.*, 29(2022), No.

2, p. 200.
[19] X.Y. Liu, F.Y. Sun, W. Wang, *et al*., Effect of chromium interlayer thickness on interfacial thermal conductance across copper/diamond interface, *Int. J. Miner. Metall. Mater.*, 29(2022), No. 11, p. 2020.
[20] G.Y. Liu, F.G. Hou, S.L. Peng, X.D. Wang, and B.Z. Fang, Process and challenges of stainless steel based bipolar plates for proton exchange membrane fuel cells, *Int. J. Miner. Metall. Mater.*, 29(2022), No. 5, p. 1099.
[21] Z. Liu, W. Cheng, D.K. Mu, *et al*., Influences of early-stage C diffusion on growth microstructures in solid-state interface reaction between CVD diamond and sputtered Cr, *Mater. Charact.*, 196(2023), art. No. 112603.
[22] H.Q. Wang, L.T. Wang, and H.Y. Zhang, The study of TiC/C composite fiber by chemical vapor deposition, *Appl. Mech. Mater.*, 69(2011), p. 99.
[23] A.P. Rubshtein, A.B. Vladimirov, Y.V. Korkh, Y.S. Ponosov, and S.A. Plotnikov, The composition, structure and surface properties of the titanium–carbon coatings prepared by PVD technique, *Surf. Coat. Technol.*, 309(2017), p. 680.
[24] N.Q. Chen, Q. Li, Y.C. Ma, *et al*., Significant strengthening of copper-based composites using boron nitride nanotubes, *Int. J. Miner. Metall. Mater.*, 30(2023), No. 9, p. 1764.
[25] Y. Huang, J.M. Ni, X.Y. Shi, *et al*., Two-step thermal transformation of multilayer graphene using polymeric carbon source assisted by physical vapor deposited copper, *Materials*, 16(2023), No. 16, art. No. 5603.
[26] X. Liu and S. Zhang, Low-temperature preparation of titanium carbide coatings on graphite flakes from molten salts, *J. Am. Ceram. Soc.*, 91(2008), No. 2, p. 667.
[27] X.G. Liu, Z.F. Wang, and S.W. Zhang, Molten salt synthesis and characterization of titanium carbide-coated graphite flakes for refractory castable applications, *Int. J. Appl. Ceram. Technol.*, 8(2011), No. 4, p. 911.
[28] J. Ding, D. Guo, C.J. Deng, H.X. Zhu, and C. Yu, Low-temperature synthesis of nanocrystalline ZrC coatings on flake graphite by molten salts, *Appl. Surf. Sci.*, 407(2017), p. 315.
[29] S. Masoudifar, M. Bavand-Vandchali, F. Golestani-Fard, and A. Nemati, Molten salt synthesis of a SiC coating on graphite flakes for application in refractory castables, *Ceram. Int.*, 42(2016), No. 10, p. 11951.
[30] Z.J. Dong, X.K. Li, G.M. Yuan, *et al*., Fabrication of protective tantalum carbide coatings on carbon fibers using a molten salt method, *Appl. Surf. Sci.*, 254(2008), No. 18, p. 5936.
[31] S. Suasmoro, F.A.R. Wati, and N. Muhaimin, Ti–Zr coating on graphite through powder immersion reaction-assisted coating (PIRAC) and its oxidation kinetics at T =1000°C, *Bull. Mater. Sci.*, 42(2019), No. 3, art. No. 126.
[32] L.H. Wang, J.W. Li, L.Y. Gao, *et al*., Gradient interface formation in Cu–Cr/diamond(Ti) composites prepared by gas pressure infiltration, *Vacuum*, 206(2022), art. No. 111549.
[33] L. Constantin, L. Fan, M. Pouey, *et al*., Spontaneous formation of multilayer refractory carbide coatings in a molten salt media, *PNAS*, 118(2021), No. 18, art. No. e2100663118.
[34] F. Behboudi, M.G. Kakroudi, N.P. Vafa, M. Faraji, and S.S. Milani, Molten salt synthesis of *in situ* TiC coating on graphite flakes, *Ceram. Int.*, 47(2021), No. 6, p. 8161.
[35] X.L. Xi, M. Feng, L.W. Zhang, and Z.R. Nie, Applications of molten salt and progress of molten salt electrolysis in secondary metal resource recovery, *Int. J. Miner. Metall. Mater.*, 27(2020), No. 12, p. 1599.
[36] J.T. Wang, X.Q. Kan, Z.L. Liu, *et al*., Low-temperature and efficient preparation of starfish-like Mo_2C/C composites from waste biomass, *J. Phys. Chem. Solids*, 181(2023), art. No. 111522.
[37] M.E. Straumanis, S.T. Shih, and A.W. Schlechten, The mechanism of deposition of titanium coatings from fused salt baths, *J. Electrochem. Soc.*, 104(1957), No. 1, art. No. 17.
[38] A. Miriyev, M. Sinder, and N. Frage, Thermal stability and growth kinetics of the interfacial TiC layer in the Ti alloy/carbon steel system, *Acta Mater.*, 75(2014), p. 348.
[39] M.I. De Barros, D. Rats, L. Vandenbulcke, and G. Farges, Influence of internal diffusion barriers on carbon diffusion in pure titanium and Ti–6Al–4V during diamond deposition, *Diam. Relat. Mater.*, 8(1999), No. 6, p. 1022.
[40] K. Kōyama, Y. Hashimoto, and S.I. Ōmori, Diffusion of carbon in TiC, *Trans. JIM*, 16(1975), No. 4, p. 211.